Journal of Thermal Analysis and Calorimetry, Vol. 77 (2004) 65–73

PHASE EQUILIBRIA IN THE SYSTEM $NiO–V_2O_5–Fe_2O_3$ IN SUBSOLIDUS AREA

Maria Kurzawa and Anna Blonska-Tabero*

Institute of Chemistry and Environment Protection, Technical University of Szczecin,
al. Piastow 42, 71-065 Szczecin, Poland

Abstract

Reactivity of $FeVO_4$ towards $Ni_2V_2O_7$ and $Ni_3V_2O_8$ in the solid state was investigated. On the base of XRD and DTA results, phase diagrams in subsolidus area of the $FeVO_4–Ni_2V_2O_7$ and $FeVO_4–Ni_3V_2O_8$ intersections of the ternary system $NiO–V_2O_5–Fe_2O_3$ have been worked out and the phase diagram of this ternary system in subsolidus area in the whole component concentration range has been verified.

Keywords: DTA, $NiO–V_2O_5–Fe_2O_3$ system, phase equilibria, XRD

Introduction

Literature reports have made it known that $FeVO_4$ as well as ortho- and divanadates(V) of divalent metals catalyse oxidation reactions of a series of organic compounds [1–4]. From this point of view the ternary system $NiO–V_2O_5–Fe_2O_3$ presents itself as an interesting research object, because within it not only the above-mentioned ortho- and divanadates(V) are formed, but also – some phases involving three oxides in their formation, namely Ni_2FeVO_6 and $Ni_2FeV_3O_{11}$ [5, 6]. These compounds are being formed as a result of a reaction between $FeVO_4$ and NiO or $FeVO_4$ and $Ni_2V_2O_7$. Therefore one may expect that they also will display interesting catalytic properties. We presented their closer characteristics and basic crystallographic data in the work [6]. Phase relations in the system $NiO–V_2O_5–Fe_2O_3$ in the whole component concentration range were a subject of research conducted by Melentev *et al.* [5]. Results of our preliminary testing investigations [7] indicate that the dividing of subsolidus area of the $NiO–V_2O_5–Fe_2O_3$ system should be made in a little other way than that proposed by previous authors [5].

The work presented herewith is a continuation of our investigations aimed at learning the reactivity in the solid state between $FeVO_4$ and $Ni_2V_2O_7$ as well as $FeVO_4$ and $Ni_3V_2O_8$, working out the phase diagrams in subsolidus area for the intersections $FeVO_4–Ni_2V_2O_7$ and $FeVO_4–Ni_3V_2O_8$ of the ternary system and a final veri-

* Author for correspondence: E-mail: mjkurzawa@ps.pl

1388–6150/2004/ $ 20.00

Akadémiai Kiadó, Budapest
Kluwer Academic Publishers, Dordrecht

fication of the phase diagram in subsolidus area of the system NiO–V_2O_5–Fe_2O_3 in the whole component concentration range.

Experimental

The reagents used for research were: NiO (99%, Aldrich, Germany), V_2O_5 (p.a., Riedel-de Haën, Germany), Fe_2O_3 (p.a., POCh, Poland) and the separately obtained phases $FeVO_4$, $Ni_2V_2O_7$ and $Ni_3V_2O_8$ prepared by heating the stoichiometric mixtures of appropriate oxides in the following cycles:

- synthesis of $FeVO_4$: 560°C(20 h)+590°C(20 h)×2
- synthesis of $Ni_2V_2O_7$: 600°C(20 h)+650°C(20 h)
- synthesis of $Ni_3V_2O_8$: 600°C(20 h)+700°C(20 h)+750°C(20 h)+780°C(20 h)

The reactions were performed by conventional sintering method. Appropriate portions of reacting substances were homogenised by grinding, shaped into pellets and heated in air for several stages until the state of equilibrium was attained. On each heating stage the samples were cooled while still in furnace to ambient temperature, ground and examined by XRD method. The heating temperatures were chosen on the base of DTA curves of selected samples.

The kind of phases occurring in the samples was always determined on the ground of their powder diffraction patterns, obtained by means of an X-ray diffractometer DRON-3 (Bourevestnik, Sankt Petersburg, Russia). A source of radiation used was a cobalt tube (CoK_α) equipped with an iron filter. The phase identification was performed on the base of X-ray characteristics contained in the PDF cards [8] and the data published in the works [5, 6, 9].

The DTA investigations were conducted by using a Paulik–Paulik–Erdey type derivatograph (MOM, Hungary). The measurements were performed in the atmosphere of air, in the temperature range 20–1000°C. Portions of 500 mg by mass were heated in quartz crucibles at a rate of 10°C/min. Accuracy of reading the temperatures of thermal effects on DTA curves, as determined by repetitions, amounted to ±5°C.

Phase diagrams were constructed on the ground of XRD and DTA results for samples at equilibrium [10–12]. The temperatures of solidus line were established on the base of the onset temperatures of first endothermic effects recorded in DTA curves of suitable samples.

Results and discussion

In order to investigate the reactions occurring in the solid state between $FeVO_4$ and $Ni_2V_2O_7$, six mixtures were prepared from separately obtained $FeVO_4$ and $Ni_2V_2O_7$. Table 1 lists the composition of initial mixtures, their heating conditions and results of XRD analysis for samples after the last heating stage.

It can be concluded from the data compiled in Table 1 that iron(III) orthovanadate(V) and nickel(II) divanadate(V) are not inert towards each other. An XRD analysis of samples containing up to ~50.00 mol% $Ni_2V_2O_7$ in their initial mixtures

Table 1 The system $FeVO_4$–$Ni_2V_2O_7$. Composition of initial mixtures, their heating conditions and XRD analysis results for samples after final heating stage

No.	Composition of initial mixtures/mol%		Heating conditions	Detected phases
	$FeVO_4$	$Ni_2V_2O_7$		
1	90.91	9.09	640°C(20 h)+780°C(20 h)×2	$Ni_2FeV_3O_{11}$, $FeVO_4$
2	76.92	23.08		
3	66.67	33.33		
4	50.00	50.00		$Ni_2FeV_3O_{11}$
5	35.00	65.00		$Ni_2FeV_3O_{11}$, $Ni_2V_2O_7$
6	15.00	85.00		

proved that they consisted of a mixture of two solid phases, $Ni_2FeV_3O_{11}$ and $FeVO_4$. It is thus evident that in this composition range of reacting substances nickel(II) divanadate(V) reacts until completion with $FeVO_4$, according to the equation:

$$FeVO_{4(s)}+Ni_2V_2O_{7(s)}=Ni_2FeV_3O_{11(s)} \quad (1)$$

The excess of $FeVO_4$ remains at equilibrium with the product of reaction (1), i.e. $Ni_2FeV_3O_{11}$. Corroboration for stating a quantitative course till completion of reaction (1) is the sample composition found after heating an equimolar mixture of $FeVO_4$ and $Ni_2V_2O_7$ (Table 1). In the remaining concentration range, *i.e.* above 50.00 mol% $Ni_2V_2O_7$ in the initial mixtures, according to the Eq. (1), the reacting substance occurring in excess is $Ni_2V_2O_7$. In this concentration range, phases coexisting at equilibrium are $Ni_2FeV_3O_{11}$ and $Ni_2V_2O_7$.

On the ground of the obtained DTA and XRD results for samples at equilibrium, a phase diagram of the system $FeVO_4$–$Ni_2V_2O_7$ in subsolidus area was constructed.

The diagram presented in Fig. 1 implies that the $FeVO_4$–$Ni_2V_2O_7$ system is a real binary system in subsolidus area in the whole component concentration range. A compound of $Ni_2FeV_3O_{11}$ crystallises in this system.

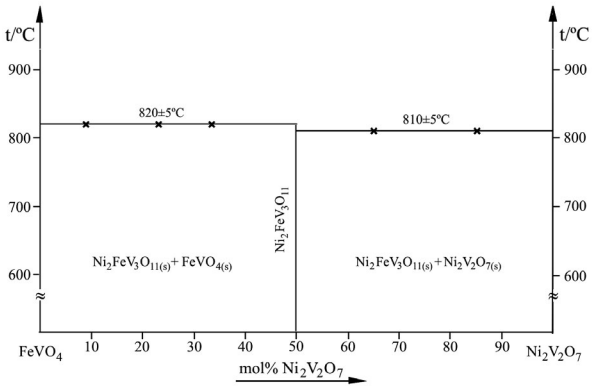

Fig. 1 Phase diagram of the system $FeVO_4$ – $Ni_2V_2O_7$ in subsolidus area

For getting knowledge on how $FeVO_4$ behaves in the solid state towards $Ni_3V_2O_8$, thirteen mixtures were prepared from separately obtained $FeVO_4$ and $Ni_3V_2O_8$. Table 2 lists the composition of initial mixtures, their heating conditions and XRD analysis results for samples after the last heating stage.

Table 2 The system $FeVO_4$ – $Ni_3V_2O_8$. Composition of initial mixtures, their heating conditions and XRD analysis results for samples after the final heating stage

No.	Composition of initial mixtures/mol%		Heating conditions	Detected phases
	$FeVO_4$	$Ni_3V_2O_8$		
1	93.33	6.67	700°C(20 h)+ 780°C(20 h)×2	$Ni_2FeV_3O_{11}$, Fe_2O_3, $FeVO_4$
2	88.89	11.11		
3	77.78	22.22		$Ni_2FeV_3O_{11}$, Fe_2O_3, $FeVO_4$ - traces
4	71.43	28.57	700°C(20 h)+780°C (20 h)+820°C(20 h)×2	$Ni_2FeV_3O_{11}$, Fe_2O_3
5	69.23	30.77		$Ni_2FeV_3O_{11}$, Fe_2O_3, $NiFe_2O_4$
6	66.67	33.33		$Ni_2FeV_3O_{11}$, $NiFe_2O_4$
7	65.38	34.62		$Ni_2FeV_3O_{11}$, Ni_2FeVO_6, $NiFe_2O_4$
8	62.41	37.59		
9	60.00	40.00	700°C(20 h)+740°C (20 h)+840°C(20 h)×2	$Ni_2FeV_3O_{11}$, Ni_2FeVO_6
10	50.00	50.00		
11	37.00	63.00		$Ni_2FeV_3O_{11}$, Ni_2FeVO_6, $Ni_3V_2O_8$
12	20.32	79.68		
13	14.29	85.71		$Ni_2FeV_3O_{11}$, $Ni_3V_2O_8$, Ni_2FeVO_6 - traces

The data presented in Table 2 imply that iron(III) orthovanadate(V) and nickel(II) orthovanadate(V) react with each other in the solid-state and the kind of yielded products depends on the composition of initial mixtures.

In the composition range of reacting substances up to ~28.57 mol% $Ni_3V_2O_8$ nickel(II) orthovanadate(V) reacts till completion with $FeVO_4$, according to the reaction equation:

$$5FeVO_{4(s)}+2Ni_3V_2O_{8(s)}=3Ni_2FeV_3O_{11(s)}+Fe_2O_{3(s)} \quad (2)$$

In this concentration range of the components, phases coexisting at equilibrium are three, $Ni_2FeV_3O_{11}$, Fe_2O_3 and $FeVO_4$. At the molar ratio of $FeVO_4/Ni_3V_2O_8$ equal to 5:2 the reaction (2) occurs quantitatively till completion (Table 2). In the concentration range of reacting substances from ~28.57 to ~33.33 mol% $Ni_3V_2O_8$ the products of reaction (2) coexist at equilibrium with $NiFe_2O_4$. This means that in this component concentration range a reaction takes place as a result of which the phase $NiFe_2O_4$ is formed. The composition of sample obtained after heating a mixture com-

prising 66.67 mol% $FeVO_4$ and 33.33 mol% $Ni_3V_2O_8$ proves that this reaction occurs quantitatively according to the equation:

$$6FeVO_{4(s)}+3Ni_3V_2O_{8(s)}=4Ni_2FeV_3O_{11(s)}+NiFe_2O_{4(s)} \quad (3)$$

When increasing the content of $Ni_3V_2O_8$ in the initial mixtures, a phase detected always in samples at equilibrium, beside the reaction (3) products, *i.e.* $Ni_2FeV_3O_{11}$ and $NiFe_2O_4$, was Ni_2FeVO_6. These three phases coexist at equilibrium in the component concentration range from ~33.33 to ~40.00 mol% $Ni_3V_2O_8$ in the initial mixtures. In this concentration range of reacting substances a reaction takes place, it appears, as a result of which the phase Ni_2FeVO_6 is formed. The composition of sample obtained after heating a mixture comprising 60.00 mol% $FeVO_4$ and 40.00 mol% $Ni_3V_2O_8$ indicates that these compounds react with each other till completion, which can be expressed by the equation:

$$3FeVO_{4(s)}+2Ni_3V_2O_{8(s)}=2Ni_2FeV_3O_{11(s)}+Ni_2FeVO_{6(s)} \quad (4)$$

In the remaining component concentration range, *i.e.* above 40.00 mol% $Ni_3V_2O_8$ in the initial mixtures, phases coexisting at equilibrium are the products of reaction (4) and $Ni_3V_2O_8$.

On the base of DTA and XRD analysis results for samples at equilibrium a phase diagram of the system $FeVO_4$–$Ni_3V_2O_8$ up to solidus line was constructed (Fig. 2).

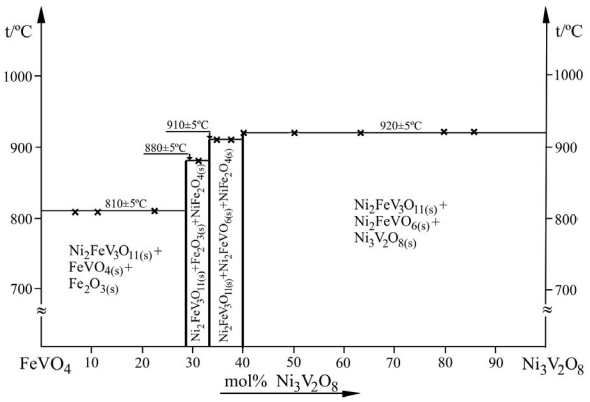

Fig. 2 Phase diagram of the system $FeVO_4$ – $Ni_3V_2O_8$ up to solidus line

It can be inferred from the diagram presented in Fig. 2 that the system $FeVO_4$–$Ni_3V_2O_8$ in the whole component concentration range is not a real binary system, but only an intersection crossing the following subsidiary subsystems of the ternary system NiO–V_2O_5–Fe_2O_3:

- $Ni_2FeV_3O_{11}$–Fe_2O_3–$FeVO_4$
- $Ni_2FeV_3O_{11}$–Fe_2O_3–$NiFe_2O_4$
- $Ni_2FeV_3O_{11}$–$NiFe_2O_4$–Ni_2FeVO_6
- $Ni_2FeV_3O_{11}$–Ni_2FeVO_6–$Ni_3V_2O_8$

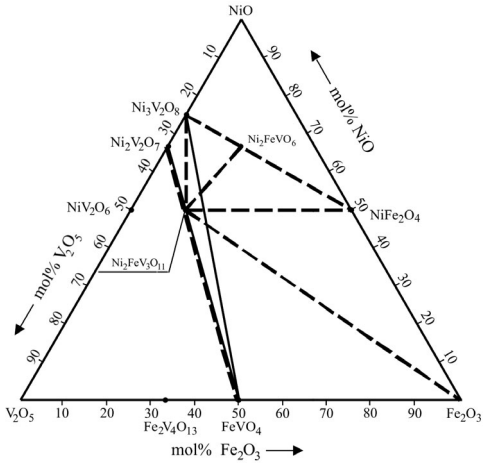

Fig. 3 Investigated intersections of the system NiO–V_2O_5–Fe_2O_3 (solid lines) and preliminary division of its subsolidus area into subsidiary subsystems (dashed lines)

Table 3 The system NiO–V_2O_5–Fe_2O_3. Composition of verifying mixtures, their heating conditions and XRD analysis results of samples after the final heating stage

No.	Composition of initial mixtures /mol%			Heating conditions	Detected phases
	NiO	V_2O_5	Fe_2O_3		
1	25.00	65.00	10.00	590°C(20 h)×6	$Fe_2V_4O_{13}$, V_2O_5, NiV_2O_6
2	25.00	55.00	20.00		$Ni_2FeV_3O_{11}$, $Fe_2V_4O_{13}$, NiV_2O_6
3	40.00	45.00	15.00		
4	25.00	50.00	25.00	590°C(20 h)×4 +620°C(20 h)×2	$Ni_2FeV_3O_{11}$, $Fe_2V_4O_{13}$, $FeVO_4$
5	33.33	44.45	22.22		
6	55.00	40.00	5.00		$Ni_2FeV_3O_{11}$, NiV_2O_6, $Ni_2V_2O_7$
7	65.00	32.00	3.00	590°C(20 h)×4 +750°C(20 h)×2	$Ni_2FeV_3O_{11}$, $Ni_2V_2O_7$, $Ni_3V_2O_8$
8	80.00	15.00	5.00	590°C(20 h)×2+660°C(20 h) +860°C(20 h)×2	NiO, $Ni_3V_2O_8$, Ni_2FeVO_6
9	65.00	10.00	25.00	590°C(20 h)×2+740°C(20 h) +860°C(20 h)×2	$NiFe_2O_4$, NiO, Ni_2FeVO_6
10	55.00	10.00	35.00	590°C(20 h)×2+620°C(20 h) +780°C(20 h)+860°C(20 h)×2	$Ni_2FeV_3O_{11}$, Ni_2FeVO_6, $NiFe_2O_4$
11	25.00	10.00	65.00	590°C(20 h)×2 + 620°C(20 h)×2 +770°C(20 h) + 820°C(20 h)×2	$Ni_2FeV_3O_{11}$, Fe_2O_3, $NiFe_2O_4$
12	40.00	43.33	16.67	590°C(20 h)×4+620°C(20 h)×5	$Ni_2FeV_3O_{11}$, $Fe_2V_4O_{13}$

Information contained in the diagrams of phase equilibria being established in the intersections $FeVO_4$–$Ni_2V_2O_7$ and $FeVO_4$–$Ni_3V_2O_8$ allowed a preliminary dividing of the subsolidus area of the NiO–V_2O_5–Fe_2O_3 system into subsidiary subsystems (Fig. 3).

The proposed division did not embrace the polygons labelled by the compounds: [NiO, $Ni_3V_2O_8$, Ni_2FeVO_6, $NiFe_2O_4$] and [$Ni_2V_2O_7$, NiV_2O_6, V_2O_5, $Fe_2V_4O_{13}$, $FeVO_4$, $Ni_2FeV_3O_{11}$].

For establishing the phase relations in these polygons twelve additional mixtures of oxides NiO, V_2O_5 and Fe_2O_3 were prepared with their compositions corresponding to those areas of the ternary system that had not been investigated and to expected subsidiary subsystems. Table 3 lists the composition of initial mixtures, their heating conditions and XRD analysis results for samples obtained after the last heating stage.

On the ground of the obtained results a phase diagram of the system NiO–V_2O_5–Fe_2O_3 in subsolidus area was worked out. Figure 4 presents a projection of the solidus surface onto the plane of the component concentration triangle of the investigated system. The melting temperatures of phase mixtures existing at equilibrium in given areas were read in each case as the onset temperature of the first endothermic effect recorded in the DTA curve of given sample.

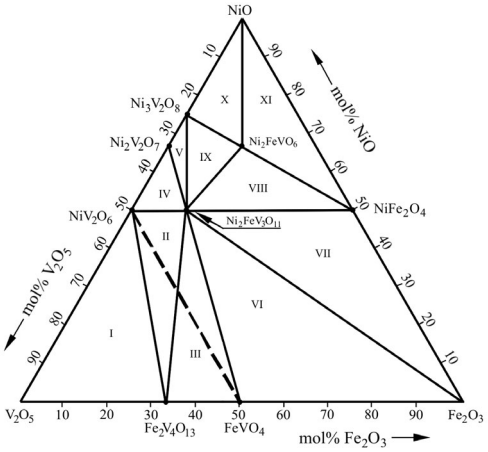

Fig. 4 Projection of solidus surface onto the plane of component concentration triangle of the system NiO–V_2O_5–Fe_2O_3 (solid lines) and according to [5] – dashed line

The presented diagram implies that in the system NiO–V_2O_5–Fe_2O_3 eleven subsidiary subsystems can be distinguished, each with three solid phases coexisting at equilibrium inside it. These are the following subsidiary subsystems:

I	V_2O_5–$Fe_2V_4O_{13}$–NiV_2O_6	melting temperature	= 620±5°C
II	NiV_2O_6–$Fe_2V_4O_{13}$–$Ni_2FeV_3O_{11}$	melting temperature	= 655±5°C
III	$Fe_2V_4O_{13}$–$FeVO_4$–$Ni_2FeV_3O_{11}$	melting temperature	= 645±5°C
IV	NiV_2O_6–$Ni_2FeV_3O_{11}$–$Ni_2V_2O_7$	melting temperature	= 690±5°C

V	$Ni_2V_2O_7$–$Ni_2FeV_3O_{11}$–$Ni_3V_2O_8$	melting temperature	= 790±5°C
VI	$FeVO_4$–Fe_2O_3–$Ni_2FeV_3O_{11}$	melting temperature	= 810±5°C
VII	$Ni_2FeV_3O_{11}$–Fe_2O_3–$NiFe_2O_4$	melting temperature	= 880±5°C
VIII	$Ni_2FeV_3O_{11}$–$NiFe_2O_4$–Ni_2FeVO_6	melting temperature	= 910±5°C
IX	$Ni_2FeV_3O_{11}$–$Ni_3V_2O_8$–Ni_2FeVO_6	melting temperature	= 920±5°C
X	$Ni_3V_2O_8$–NiO–Ni_2FeVO_6	melting temperature	> 1000°C
XI	Ni_2FeVO_6–NiO–$NiFe_2O_4$	melting temperature	> 1000°C

The phase diagram of the system NiO–V_2O_5–Fe_2O_3 presented in Fig. 4 differs a little from the diagram worked out by previous authors [5]. Dashed line in Fig. 4 denotes the subsidiary subsystems proposed by Melentev *et al.*, that is [NiV_2O_6–$Fe_2V_4O_{13}$–$FeVO_4$] and [$FeVO_4$–NiV_2O_6–$Ni_2FeV_3O_{11}$]. In the system NiO – V_2O_5–Fe_2O_3 no formation of solid solutions was revealed either – the existence of which was reported in the work [5].

Figure 5 presents a perspective view of the subsolidus area of the system NiO–V_2O_5–Fe_2O_3.

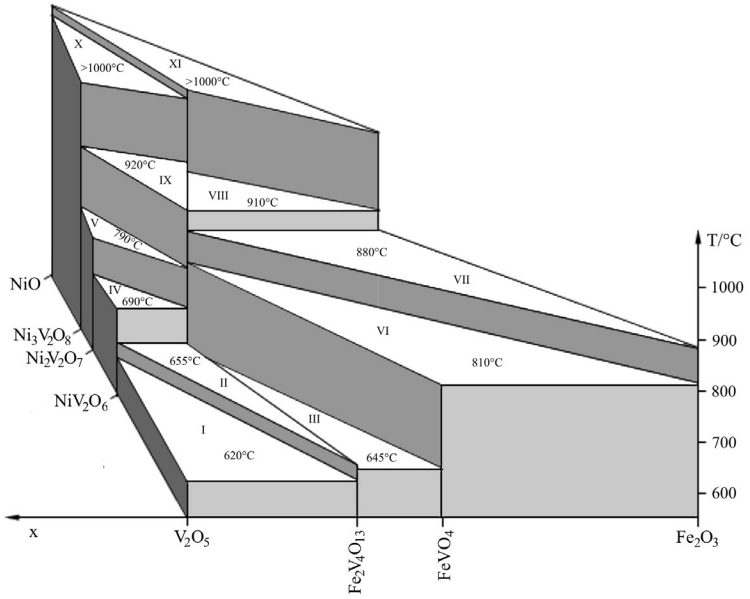

Fig. 5 Perspective view of subsolidus area of the system NiO–V_2O_5–Fe_2O_3

Conclusions

- The $FeVO_4$ – $Ni_2V_2O_7$ system is a real binary system in subsolidus area in the whole component concentration range.

- The $FeVO_4$ – $Ni_3V_2O_8$ system in the whole component concentration range is an intersection crossing 4 subsidiary subsystems of the ternary system NiO – V_2O_5–Fe_2O_3.
- 11 subsidiary subsystems can be distinguished in the NiO–V_2O_5 – Fe_2O_3 system, in which three solid phases co-exist at equilibrium in every case.

References

1 B. Zhaorigetu, W. Li, R. Kieffer and H. Xu, React. Kinet. Catal. Lett., 75 (2002) 275.
2 S. A. Korili, P. Ruiz and B. Delmon, Catalysis Today, 32 (1996) 229.
3 W. S. Chang, Y. Z. Chen and B. L. Yang, Appl. Catal., A, 124 (1995) 221.
4 L. N. Kurina and L. M. Potalitsyna, Izv. Vyssh. Uchebn. Zaved., Khim. Khim. Tekhnol., 26 (1983) 1218.
5 A. B. Melentev, L. L. Surat, A. A. Fotiev, G. A. Suvorova and T. P. Sirina, Zh. Neorg. Khim., 33 (1988) 2149.
6 M. Kurzawa, A. Blonska-Tabero, I. Rychłowska-Himmel and P. Tabero, Mat. Res. Bull., 36 (2001) 1379.
7 J. Walczak, I. Rychłowska-Himmel and A. Blonska-Tabero, 36th IUPAC Congress, Geneva 1997 (Switzerland), Chimia, 51 (1997) 402.
8 Powder Diffraction File, International Center for Diffraction Data, Swarthmore (USA), File Nos.: 9-387, 33-664, 22-1189, 38-1372, 39-893, 10-325, 38-0285, 37-353.
9 A. Le Bail and M.-A. Lafontaine, Eur. J. Solid State Inorg. Chem., 27 (1990) 671.
10 D. Živkovic, I. Katayama, A. Kostov and Ž. Živkovic, J. Therm. Anal. Cal., 71 (2003) 567.
11 M. Ferretti and E. Magnone, J. Therm. Anal. Cal., 70 (2002) 129.
12 I. Rychłowska-Himmel and P. Tabero, J. Therm. Anal. Cal., 65 (2001) 537.